the membrane with a white noise–driven piezoelectric actuator (purple trace exceeds dashed curve in Fig. 3B), which also drives mechanical modes of the mirrors and supports, leading to extra modulation. However, the cross-correlation spectrum (blue trace) remains unchanged, equal to the unperturbed spectrum (dashed curve), implying that very little of the ambient motion is transduced.

The cross-correlation can also be viewed as evidence that we have made a quantum nondemolition (QND) measurement of the intracavity photon fluctuations of the signal beam (*14*, *28*). Here, the membrane acts as the measurement device, with its state of motion recording the photon fluctuations over the band of the mechanical resonance. The correlation C is equivalent to a state preparation fidelity for a nonideal QND measurement (*29*). Further, it has been shown that frequency-dependent ponderomotive squeezing of the signal beam quantum noise is possible (*30*) and has recently been demonstrated in an atomic gas cavity optomechanical system (*31*). For our current laser configuration ($\Delta_S = 0$), we do not expect to see squeezing in the detected amplitude quadrature. However, our device parameters are sufficient to realize much stronger squeezing than has previously been demonstrated, limited mainly by optical loss. Our observations open the door to realizing position measurement near the SQL if residual thermal noise and excess cavity-laser phase noise can be eliminated with improved devices or a colder base temperature.

References and Notes

1. G. M. Harry, *Class. Quantum Gravity* **27**, 084006 (2010).
2. V. Braginsky, S. Vyatchanin, *Sov. Phys. JETP* **47**, 433 (1978).
3. C. M. Caves, *Phys. Rev. D Part. Fields* **23**, 1693 (1981).
4. K. Somiya, *Class. Quantum Gravity* **29**, 124007 (2012).
5. H. J. Kimble, Y. Levin, A. B. Matsko, K. S. Thorne, S. P. Vyatchanin, *Phys. Rev. D Part. Fields* **65**, 022002 (2001).
6. V. B. Braginsky, Y. I. Vorontsov, K. S. Thorne, *Science* **209**, 547 (1980).
7. J. D. Teufel, T. Donner, M. A. Castellanos-Beltran, J. W. Harlow, K. W. Lehnert, *Nat. Nanotechnol.* **4**, 820 (2009).
8. G. Anetsberger *et al.*, *Phys. Rev. A* **82**, 061804 (2010).
9. D. M. Stamper-Kurn, in *Cavity Optomechanics*, M. Aspelmeyer, T. Kippenberg, F. Marquardt, Eds. (Springer, New York); preprint available at http://arxiv.org/abs/1204.4351.
10. K. W. Murch, K. L. Moore, S. Gupta, D. M. Stamper-Kurn, *Nat. Phys.* **4**, 561 (2008).
11. I. Tittonen *et al.*, *Phys. Rev. A* **59**, 1038 (1999).
12. P. Verlot *et al.*, *C. R. Phys.* **12**, 826 (2011).
13. P. Verlot, A. Tavernarakis, T. Briant, P.-F. Cohadon, A. Heidmann, *Phys. Rev. Lett.* **102**, 103601 (2009).
14. A. Heidmann, Y. Hadjar, M. Pinard, *Appl. Phys. B* **64**, 173 (1997).
15. K. Børkje *et al.*, *Phys. Rev. A* **82**, 013818 (2010).
16. K. Yamamoto *et al.*, *Phys. Rev. A* **81**, 033849 (2010).
17. A. Naik *et al.*, *Nature* **443**, 193 (2006).
18. J. D. Teufel *et al.*, *Nature* **475**, 359 (2011).
19. J. Chan *et al.*, *Nature* **478**, 89 (2011).
20. E. Verhagen, S. Deléglise, S. Weis, A. Schliesser, T. J. Kippenberg, *Nature* **482**, 63 (2012).
21. F. Y. Khalili *et al.*, *Phys. Rev. A* **86**, 033840 (2012).
22. A. H. Safavi-Naeini *et al.*, *Phys. Rev. Lett.* **108**, 033602 (2012).
23. T. P. Purdy, R. W. Peterson, P.-L. Yu, C. A. Regal, *New J. Phys.* **14**, 115021 (2012).
24. J. D. Thompson *et al.*, *Nature* **452**, 72 (2008).
25. F. Marquardt, J. P. Chen, A. A. Clerk, S. M. Girvin, *Phys. Rev. Lett.* **99**, 093902 (2007).
26. Materials and methods are available as supplementary materials on *Science* Online.
27. I. Wilson-Rae, N. Nooshi, W. Zwerger, T. J. Kippenberg, *Phys. Rev. Lett.* **99**, 093901 (2007).
28. K. Jacobs, P. Tombesi, M. J. Collett, D. F. Walls, *Phys. Rev. A* **49**, 1961 (1994).
29. M. J. Holland, M. J. Collett, D. F. Walls, M. D. Levenson, *Phys. Rev. A* **42**, 2995 (1990).
30. C. Fabre *et al.*, *Phys. Rev. A* **49**, 1337 (1994).
31. D. W. C. Brooks *et al.*, *Nature* **488**, 476 (2012).

Acknowledgments: We thank P.-L. Yu for technical assistance and K. Lehnert's group for helpful discussions. This work is supported by: the Defense Advanced Research Projects Agency Quantum-Assisted Sensing and Readout program, the Office of Naval Research Young Investigator Program, and the JILA NSF Physics Frontier Center. T.P.P. thanks the National Research Council for support. C.A.R. thanks the Clare Boothe Luce foundation for support.

Supplementary Materials

www.sciencemag.org/cgi/content/full/339/6121/801/DC1
Materials and Methods
Figs. S1 to S5
References (*32*, *33*)

9 October 2012; accepted 18 December 2012
10.1126/science.1231282

Similarity of Scattering Rates in Metals Showing *T*-Linear Resistivity

J. A. N. Bruin,[1] H. Sakai,[1] R. S. Perry,[2] A. P. Mackenzie[1]

Many exotic compounds, such as cuprate superconductors and heavy fermion materials, exhibit a linear in temperature (T) resistivity, the origin of which is not well understood. We found that the resistivity of the quantum critical metal $Sr_3Ru_2O_7$ is also T-linear at the critical magnetic field of 7.9 T. Using the precise existing data for the Fermi surface topography and quasiparticle velocities of $Sr_3Ru_2O_7$, we show that in the region of the T-linear resistivity, the scattering rate per kelvin is well approximated by the ratio of the Boltzmann constant to the Planck constant divided by 2π. Extending the analysis to a number of other materials reveals similar results in the T-linear region, in spite of large differences in the microscopic origins of the scattering.

When the high-temperature cuprate superconductors were discovered, it quickly became clear that the highest superconducting transition temperatures were seen in materials whose electrical resistivity varied linearly with temperature (T) in certain regions of the temperature-doping phase diagram. Since then, T-linear resistivity has been seen in the pnictide and organic superconductors, as well as in many heavy fermion compounds, both superconducting and non-superconducting. In most of the heavy fermion materials, the T-linear resistivity is seen when they have been tuned by some external parameter to create a low-temperature continuous phase transition known as a quantum critical point (QCP). T-linear resistivity is therefore often associated with quantum criticality. However, other power laws—for example, $T^{1.5}$—are also seen in the resistivity in quantum critical systems (*1*), and the origin of the T-linear term remains the subject of active research and debate. Here, we present an analysis of electrical transport data from 1.5 to 400 K in $Sr_3Ru_2O_7$ and compare our findings to those in a wide variety of other materials, including elemental metals, that exhibit T-linear resistivity.

$Sr_3Ru_2O_7$ is a magnetic-field–tuned quantum critical system (*2*) that can be prepared in single-crystal form with very low levels of disorder (*3*, *4*). For an applied field oriented parallel to the crystallographic c axis, the approach to the quantum critical point at the critical field $\mu_o H_c = 7.9$ T is cut off by the formation of a purity-sensitive nematic phase for $7.8\ \mathrm{T} < \mu_o H < 8.1\ \mathrm{T}$ and $T < 1.2$ K. Outside this phase, canonical signatures of quantum criticality are seen in a range of physical properties including the spin-lattice relaxation rate, thermal expansion, specific heat, and magnetocaloric effect (*5*–*8*). As the magnetic field is varied at low temperature, both the specific heat and entropy show a strong peak, centered on H_c. Cooling at zero field shows a broad peak in the electronic specific heat coefficient $\gamma = c_{el}/T$, centered at approximately 10 K but extending to $T^* \sim 25$K. As the field is increased, this peak sharpens, and its characteristic temperature is depressed, until at H_c, γ varies as $-\ln T$ for $1.2\mathrm{K} < T < 20$ K. At all fields, an entropy of $\sim 0.1R\ln 2$ is recovered by T^*, where R is the molar gas constant (*8*). These observations indicate that the ~25K energy scale is associated with a fraction of the states in the Brillouin zone and that these states are responsible for the quantum criticality. Above T^*, they have the entropic characteristics of "classical" fluctuators at all applied fields, with the crossover temperature suppressed on the approach to H_c.

The fact that only some of the states in the Brillouin zone participate thermodynamically in the quantum criticality is consistent with findings from the de Haas-van Alphen (dHvA) effect and angle-resolved photoemission (*9*, *10*). Six distinct dHvA frequencies are identified, each corresponding to quasi–two dimensional (2D) Fermi surface pockets, and the quasiparticle masses are essentially field-independent for five of them (*9*). Thermo-

[1]Scottish Universities Physics Alliance, School of Physics and Astronomy, University of St Andrews, North Haugh, St Andrews KY16 9SS, UK. [2]Scottish Universities Physics Alliance, School of Physics and Astronomy, University of Edinburgh, Mayfield Road, Edinburgh EH9 3JZ, UK.

dynamically, therefore, $Sr_3Ru_2O_7$ can be thought of as two metallic fluids, one which participates directly in the quantum criticality and another, containing a higher density of quasiparticles, which does not.

Given the extensive knowledge of the thermodynamic and quasiparticle properties of $Sr_3Ru_2O_7$, it is natural to investigate its electrical transport properties both below and above T^* (*11*). In Fig. 1, we show the temperature evolution of the data at representative magnetic fields from across the range studied, for $T > T_c$. In zero field, ρ varies approximately quadratically with temperature for 1.2 K < T < 10 K, which is in qualitative agreement with previous reports (*2*, *12*). As the field is increased toward H_c, the temperature range over which the approximately quadratic temperature dependence occurs shrinks, until at the critical field of 7.9 T, the resistivity varies linearly with temperature over the whole range shown, with a gradient of 1.1 microhm·cm/K. For $H > H_c$ (Fig. 1B) there is a small negative magnetoresistance, but the gradient of the resistivity once it has become linear is almost independent of field.

That T-linear resistivity is seen in $Sr_3Ru_2O_7$ is surprising. As discussed above, the majority of the quasiparticles do not participate in the mass divergence at H_c. If they were simply an independent Fermi liquid contributing to the conductivity in parallel with the quantum critical fluid, they would be expected to short out the contribution of the small number of carriers that are becoming heavy on the approach to H_c, giving a dominant T^2 contribution to the resistivity. The data of Fig. 1 strongly suggest that as well as inducing a mass divergence in a subset of the carriers, the quantum criticality in $Sr_3Ru_2O_7$ is associated with the onset of efficient scattering, with strength proportional to T, which affects all the quasiparticles.

Qualitative support for this basic picture comes from the data presented in Fig. 1C, in which we show the resistivity of $Sr_3Ru_2O_7$ for the same set of fields as in Fig. 1A, but for temperatures extending to 400 K. Above 100 K, ρ is again T-linear, in this case at all applied fields, but with a gradient ~30% lower than that seen at H_c for T < 20 K. There is an interesting correlation between this observation and previous studies of the specific heat. Measurements to elevated temperatures show that for $T > T^*$, γ is field-independent and ~65% of the low temperature value measured in zero applied field (8). This implies a similar fall in the average effective mass, or equivalently, a 35% rise in the average Fermi velocity. The data in Fig. 1C therefore suggest that there is a similar scattering rate per kelvin below T^* at H_c and well above T^* at all applied fields.

Although attention is typically focused on the power law dependence of the resistivity, the absolute magnitude of the scattering rate is also an important quantity. A phenomenological argument for a T-linear scattering rate has been discussed by a number of authors in the context of the cuprates and quantum critical metals and fluids (*13*–*15*). Because quantum criticality is associated with the depression of energy scales toward $T = 0$, temperature becomes the only relevant energy scale. Equipartition of energy then applies, and the characteristic energy of any quantum critical degree of freedom is just k_BT, where k_B is Boltzmann's constant. This in turn implies the existence of a characteristic time, sometimes referred to as the Planck time $\tau_P \sim \hbar/k_BT$, where $\hbar$ is Planck's constant divided by 2π. Although the simplicity of this expression is appealing, it is far from obvious that $(T\tau_P)^{-1} \sim k_B/\hbar$ defines a scattering rate relevant to a measurement of electrical resistivity. Resistive scattering processes must relax

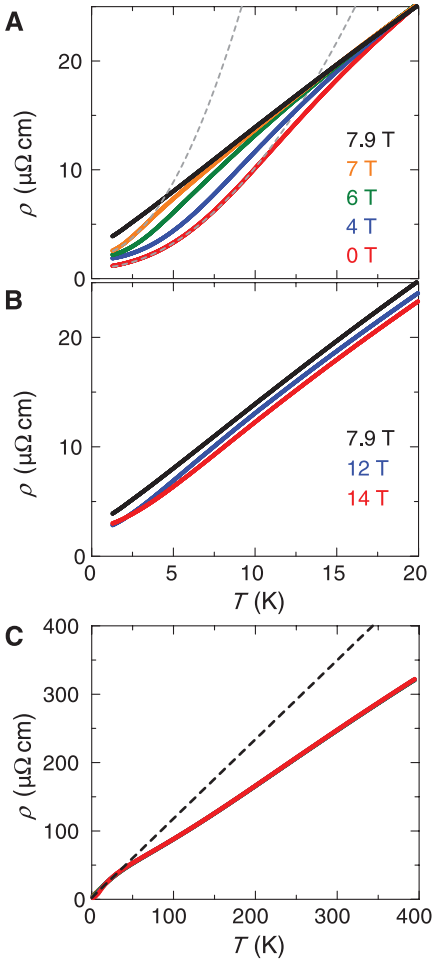

Fig. 1. (**A**) Resistivity (ρ) of high-purity single crystal $Sr_3Ru_2O_7$ at 0 T (red), 4 T (blue), 6 T (green), 7 T (orange), and its critical field μ_0H_c= 7.9 T (black). The gray dashed lines are fits of the type $\rho_0 + AT^2$ to the low-temperature data, which illustrate the suppression of the temperature at which the resistivity crosses over to being quadratic in temperature as H is tuned toward H_c. (**B**) ρ at H_c (black), 12 T (blue), and 14 T (red). (**C**) ρ at 0 T, 4 T, 6 T, 7 T, and H_c over an extended temperature range up to 400 K. Above 20 K, there is a negative magnetoresistance, but it is so small that data at all fields overlap when plotted on this scale. The dotted line shows the extrapolation of the low-temperature linear resistivity at 7.9 T.

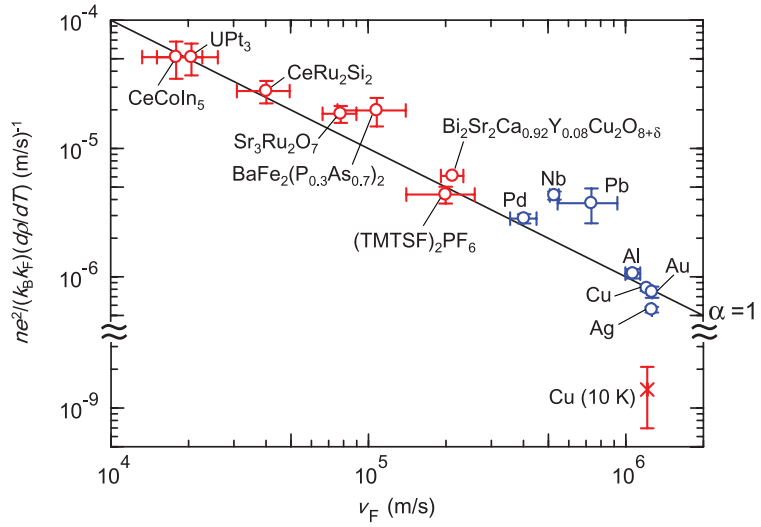

Fig. 2. In spite of two orders of magnitude variations in their Fermi velocities (v_F), a wide range of metals in which the resistivity varies linearly with temperature have similar scattering rates per kelvin. These include heavy fermion, oxide, pnictide, and organic metals for which T-linear resistivity can be seen down to low temperatures with appropriate tuning by magnetic field, chemical composition, or hydrostatic pressure, and more conventional metals for which T-linear resistivity is seen at high temperatures (blue symbols). At low temperatures, the scattering rate per kelvin of a conventional metal is orders of magnitude lower, as illustrated for the case of Cu at 10 K, shown in the lower right hand corner (*11*). On the graph, the line marked α = 1 corresponds to $(\tau T)^{-1} = k_B/h$. The near-universality of the scattering rates is observed in spite of the fact that the scattering mechanisms vary across the range of materials. The point for $Bi_2Sr_2Ca_{0.92}Y_{0.08}Cu_2O_{8+\delta}$ is based on the value α = 1.3, which is determined from optical conductivity (*21*), combined with the measured value of v_F for this material (*44*). For all others, the analysis is based on resistivity data combined with knowledge of the Fermi volume and average Fermi velocity. Full details of the determination of the parameters in the axis labels are given in (*11*).

momentum efficiently within the electronic fluid, transfer that momentum to the lattice, and ultimately dissipate energy. In other words, there is no a priori reason to expect the resistive scattering rate τ^{-1} to have either the same temperature dependence or magnitude as τ_P^{-1}. Here, we concentrate on the case in which $\tau(T) \propto \tau_P(T)$, and write $(T\tau)^{-1} \sim \alpha k_B/\hbar$, so that $\tau(T) = \tau_P(T)$ corresponds to phenomenological dimensionless constant $\alpha = 1$. We can measure α in $Sr_3Ru_2O_7$ with some confidence because it has a quasi-2D Fermi surface, and the volume and average Fermi velocity of each Fermi surface sheet have been established empirically, even for fields close to H_c (*9*). Working in a 2D isotropic-relaxation-time approximation that is useful for estimating the average scattering rate (*16*, *17*) we write

$$\frac{1}{\tau} = \frac{e^2\rho}{hd}\sum_i k_{Fi} v_{Fi} \qquad (1)$$

where e is the electronic charge, d is the bilayer-bilayer spacing of 10.35 Å, k_F is the Fermi wave vector, v_F is the Fermi velocity, and index i ensures that the sum is over all pockets, taking into account multiplicities in the Brillouin zone. We then used Eq. 1, in combination with our $\rho(T)$ data, to determine the temperature dependence of τ^{-1}. Performing the calculation using the data for $H = H_c$ and the quasiparticle parameters of (*9*) gives $\alpha = 1.5$ (*11*).

The fact that α is close to 1 in $Sr_3Ru_2O_7$ is intriguing, especially given that similar conclusions have been reached about the cuprates at optimal doping from analysis of high-frequency conductivity data (*13*, *18*–*22*), photoemission spectra (*23*), and transport measurements (*14*). Our observations therefore motivate analysis of the resistivity of other materials in which T-linear resistivity is observed. Converting resistivity data to a scattering rate requires good knowledge of Fermi volumes and Fermi velocities, close to the critical tuning parameter at which the T-linear resistivity is observed. Sufficient information for reliable analysis, usually deduced from the dHvA effect, exists for $BaFe_2(As_{1-x}P_x)_2$ (*24*, *25*), $(TMTSF)_2PF_6$ (*26*, *27*), $CeCoIn_5$ (*28*–*30*), UPt_3 (*31*, *32*), and $CeRu_2Si_2$ (*33, 34*) (the last two near their metamagnetic transitions). Across this range of strongly correlated materials, we found $0.9 < \alpha < 2.2$, in spite of pronounced differences in both their effective dimensionality [varying from quasi-1D in $(TMTSF)_2PF_6$ to 3D in UPt_3] and the microscopic nature of the interactions. Full details of the calculations, which take the dimensionality of the electronic structure into account, are given in (*11*).

A natural question posed by these observations is whether T-linear scattering at $k_B/\hbar$ per kelvin is exclusive to quantum critical systems. Central to the phenomenological argument that $(\tau T)^{-1} \sim k_B/\hbar$ is the applicability of equipartition of energy to the degree of freedom from which the quasiparticles scatter. In addition to quantum critical systems as $T \to 0$, this condition is well known to apply at high temperatures in a further class of materials in which T-linear resistivity is observed, metals in which the scattering is from phonons rather than excitations of electronic origin. Because the nature of the scattering centers is different, and the high temperature resistivity of metals such as copper, gold, and silver is two orders of magnitude lower than that of the strongly correlated materials discussed above, they are often assumed to be fundamentally different. However, the difference in the absolute value of the resistivity is accounted for by their much higher carrier concentrations and Fermi velocities, and again, $\alpha \sim 1$ [$0.7 < \alpha < 2.7$ for Ag, Au, Pd, Cu, Al, Nb, and Pb, with full analysis described in (*11*)].

The fact that the resistively determined scattering rate per kelvin is approximately $k_B/\hbar$ across such a wide range of materials is our main experimental finding. It is summarized in Fig. 2. Although the main purpose of this paper is to report this empirical fact, we close with a brief discussion of some of the issues that are raised by our observations.

The first concerns the underlying origin for T-linear resistivity in quantum critical systems. Our analysis is based on the assumption that the main effect of quantum criticality on the resistivity is to provide a quasi-classical degree of freedom from which even light, "cold" Fermi liquid quasiparticles scatter rather than to destroy all the quasiparticles. In $Sr_3Ru_2O_7$, this is the only way to understand how T-linear resistivity can be observed. Similar issues of "hot" and cold carriers have been highlighted in the context of cuprates (*35*) and heavy fermion systems (*36*). In fact, most of the other strongly correlated materials shown in Fig. 2 also have cold carriers that, in the simplest models, would short out the T-linear contribution. This seems to be strong evidence that in those materials too, all the carriers are subject to strong scattering. This analysis helps resolve a puzzle about $Sr_3Ru_2O_7$ and some other quantum critical metallic systems: The crossover to T^2 resistivity (Fig. 1) typically occurs at far lower T than the Fermi temperature (T_F) inferred from the average effective mass. If the resistive crossover is related to the characteristic energy of the quantum critical scattering, this might indeed be much lower than T_F for most of the quasiparticles.

In materials in which phonon scattering is thought to dominate, electron-phonon processes in the high temperature limit have a T-linear scattering rate that is conventionally expressed as $(\tau T)^{-1} = 2\pi\lambda k_B/\hbar$, where λ is a dimensionless coupling constant that is not thought to be universal (*37*); in the language of this paper, the phenomenological constant $\alpha = 2\pi\lambda$. The data summarized in Fig. 2, however, suggest that the coupling constant deduced from the electrical resistivity is insensitive to the detail of the scattering processes. This finding also highlights a second key feature of scattering in the strongly correlated materials. Phonon modes at high temperatures are known to have a large wave vector q and hence to be efficient at relaxing electron momentum. The near material-independence of α across electron-phonon and strongly correlated systems implies that whatever their microscopic origin, the low-temperature degrees of freedom in the strongly correlated systems must be equally efficient at high-q scattering, via normal processes, Umklapp processes, or a combination of the two. This is implicit in the data shown in Fig. 1 for $Sr_3Ru_2O_7$; the fact that the linear resistivity is seen at all in this multi-band material implies efficient scattering throughout the Brillouin zone.

A further issue raised is the effect of combining different sources of scattering in the same material. It has always seemed strange that no obvious signatures of electron-phonon scattering are seen in strongly correlated materials such as the cuprates, in which electron-electron processes are thought to dominate. Electron-phonon coupling is also expected to be strong in such materials, so electron-phonon scattering should be visible as an extra contribution to the resistivity, particularly at higher temperatures. There is very little experimental evidence for this additive contribution. One possibility raised by the data shown in Fig. 2 is that there is a universal upper limit to the rate of scattering observable in a measurement of T-linear resistivity, no matter how many sources of scattering are combined.

A final hint toward universal behavior comes from the study of quantum hydrodynamic fluids. In a hydrodynamic fluid, the shear viscosity η is inversely proportional to the scattering rate because all dissipation processes are nonlocal. Experiments have shown that when the scattering rate is T-linear, the ratio of η to entropy density s is very small, with $\eta/s \cong \hbar/2k_B$ for fluids as diverse as the quark-gluon plasma and ultra-cold ^{6}Li (*38*–*40*). Under certain assumptions $\eta/s \cong \tau T$ (*41*), so the measurements correspond to $\alpha \cong 2$, which is quantitatively similar to those reported here for electrons in metals. In the hydrodynamic fluids, calculations based on string theory predict a "minimum viscosity limit" of $\eta/s \geq \hbar/4\pi k_B$ (*42*). Hydrodynamic theory is not directly applicable to most metals (*43*), but if the essence of these calculations is the prediction of a universal bound on a T-linear scattering rate, there may prove to be relevance to the observations that we have reported here. Whatever the final explanation, the data summarized in Fig. 2 provide a novel perspective on a decades-old problem.

References and Notes

1. G. R. Stewart, *Rev. Mod. Phys.* **73**, 797 (2001).
2. S. A. Grigera *et al.*, *Science* **294**, 329 (2001).
3. R. S. Perry *et al.*, *Phys. Rev. Lett.* **92**, 166602 (2004).
4. S. A. Grigera *et al.*, *Science* **306**, 1154 (2004).
5. K. Kitagawa *et al.*, *Phys. Rev. Lett.* **95**, 127001 (2005).
6. P. Gegenwart, F. Weickert, M. Garst, R. S. Perry, Y. Maeno, *Phys. Rev. Lett.* **96**, 136402 (2006).
7. A. W. Rost, R. S. Perry, J. F. Mercure, A. P. Mackenzie, S. A. Grigera, *Science* **325**, 1360 (2009).
8. A. W. Rost *et al.*, *Proc. Natl. Acad. Sci. U.S.A.* **108**, 16549 (2011).
9. J. F. Mercure *et al.*, *Phys. Rev. B* **81**, 235103 (2010).
10. A. Tamai *et al.*, *Phys. Rev. Lett.* **101**, 026407 (2008).
11. Materials and methods are available as supplementary materials on *Science* Online.
12. L. Capogna *et al.*, *Phys. Rev. Lett.* **88**, 076602 (2002).
13. J. Zaanen, *Nature* **430**, 512 (2004).
14. R. A. Cooper *et al.*, *Science* **323**, 603 (2009).
15. T. Schäfer, D. Teaney, *Rep. Prog. Phys.* **72**, 126001 (2009).

16. N. P. Ong, *Phys. Rev. B* **43**, 193 (1991).
17. P. L. Taylor, *Proc. R. Soc. Lond. A Math. Phys. Sci.* **275**, 209 (1963).
18. J. W. Orenstein *et al.*, *Phys. Rev. B* **42**, 6342 (1990).
19. Z. Schlesinger *et al.*, *Phys. Rev. B* **41**, 11237 (1990).
20. H. L. Liu *et al.*, *J. Phys. Condens. Matter* **11**, 239 (1999).
21. D. van der Marel *et al.*, *Nature* **425**, 271 (2003).
22. C. C. Homes *et al.*, *Nature* **430**, 539 (2004).
23. T. Valla *et al.*, *Science* **285**, 2110 (1999).
24. S. Kasahara *et al.*, *Phys. Rev. B* **81**, 184519 (2010).
25. H. Shishido *et al.*, *Phys. Rev. Lett.* **104**, 057008 (2010).
26. N. Doiron-Leyraud *et al.*, *Eur. Phys. J. B* **78**, 23 (2010).
27. J. S. Brooks, *Rep. Prog. Phys.* **71**, 126501 (2008).
28. M. A. Tanatar, J. Paglione, C. Petrovic, L. Taillefer, *Science* **316**, 1320 (2007).
29. R. Settai *et al.*, *J. Phys. Condens. Matter* **13**, L627 (2001).
30. A. McCollam, S. R. Julian, P. M. C. Rourke, D. Aoki, J. Flouquet, *Phys. Rev. Lett.* **94**, 186401 (2005).
31. J. S. Kim, D. Hall, K. Heuser, G. R. Stewart, *Solid State Commun.* **114**, 413 (2000).
32. N. Kimura *et al.*, *Physica B* **281-282**, 710 (2000).
33. R. Daou, C. Bergemann, S. R. Julian, *Phys. Rev. Lett.* **96**, 026401 (2006).
34. M. Takashita *et al.*, *J. Phys. Soc. Jpn.* **65**, 515 (1996).
35. R. Hlubina, T. M. Rice, *Phys. Rev. B* **51**, 9253 (1995).
36. A. Rosch, *Phys. Rev. Lett.* **82**, 4280 (1999).
37. J. M. Ziman, *Electrons and Phonons* (Clarendon Press, Oxford, UK, 1960).
38. S. S. Adler *et al.*; PHENIX Collaboration, *Phys. Rev. Lett.* **91**, 182301 (2003).
39. T. Schäfer, *Phys. Rev. A* **76**, 063618 (2007).
40. C. Cao *et al.*, *Science* **331**, 58 (2011).
41. D. A. Teaney, *arXiv*:0905.2433v1.
42. P. K. Kovtun, D. T. Son, A. O. Starinets, *Phys. Rev. Lett.* **94**, 111601 (2005).
43. A. V. Andreev, S. A. Kivelson, B. Spivak, *Phys. Rev. Lett.* **106**, 256804 (2011).
44. A. Kaminski *et al.*, *Phys. Rev. B* **71**, 014517 (2005).

Acknowledgments: We are pleased to acknowledge the help of M. Baenitz, M. Nicklas, and C. Klausnitzer of the Max Planck Institute for the Chemical Physics of Solids in Dresden, where the high-temperature resistivity measurements on $Sr_3Ru_2O_7$ were performed, and useful discussions with J. Orenstein, S. A. Kivelson, C. A. Hooley, and J. Zaanen. The research was supported by the UK Engineering and Physical Sciences Research Council. H.S. gratefully acknowledges fellowships from the Canon Foundation Europe and Marubun Research Promotion Foundation, and A.P.M. acknowledges the receipt of a Royal Society–Wolfson Merit Award.

Supplementary Materials

www.sciencemag.org/cgi/content/full/339/6121/804/DC1
Materials and Methods
Supplementary Text
Fig. S1
Tables S1 to S10
References (*45*–*65*)

18 July 2012; accepted 27 November 2012
10.1126/science.1227612

Detection of the Characteristic Pion-Decay Signature in Supernova Remnants

M. Ackermann,[1] M. Ajello,[2] A. Allafort,[3] L. Baldini,[4] J. Ballet,[5] G. Barbiellini,[6,7] M. G. Baring,[8] D. Bastieri,[9,10] K. Bechtol,[3] R. Bellazzini,[11] R. D. Blandford,[3] E. D. Bloom,[3] E. Bonamente,[12,13] A. W. Borgland,[3] E. Bottacini,[3] T. J. Brandt,[14] J. Bregeon,[11] M. Brigida,[15,16] P. Bruel,[17] R. Buehler,[3] G. Busetto,[9,10] S. Buson,[9,10] G. A. Caliandro,[18] R. A. Cameron,[3] P. A. Caraveo,[19] J. M. Casandjian,[5] C. Cecchi,[12,13] Ö. Çelik,[14,20,21] E. Charles,[3] S. Chaty,[5] R. C. G. Chaves,[5] A. Chekhtman,[22] C. C. Cheung,[23] J. Chiang,[3] G. Chiaro,[24] A. N. Cillis,[14,25] S. Ciprini,[13,26] R. Claus,[3] J. Cohen-Tanugi,[27] L. R. Cominsky,[28] J. Conrad,[29,30,31] S. Corbel,[5,32] S. Cutini,[33] F. D'Ammando,[12,34,35] A. de Angelis,[36] F. de Palma,[15,16] C. D. Dermer,[37] E. do Couto e Silva,[3] P. S. Drell,[3] A. Drlica-Wagner,[3] L. Falletti,[27] C. Favuzzi,[15,16] E. C. Ferrara,[14] A. Franckowiak,[3] Y. Fukazawa,[38] S. Funk,[3]* P. Fusco,[15,16] F. Gargano,[16] S. Germani,[12,13] N. Giglietto,[15,16] P. Giommi,[33] F. Giordano,[15,16] M. Giroletti,[39] T. Glanzman,[3] G. Godfrey,[3] I. A. Grenier,[5] M.-H. Grondin,[40,41] J. E. Grove,[37] S. Guiriec,[14] D. Hadasch,[18] Y. Hanabata,[38] A. K. Harding,[14] M. Hayashida,[3,42] K. Hayashi,[38] E. Hays,[14] J. W. Hewitt,[14] A. B. Hill,[3,43] R. E. Hughes,[44] M. S. Jackson,[30,45] T. Jogler,[3] G. Jóhannesson,[46] A. S. Johnson,[3] T. Kamae,[3] J. Kataoka,[47] J. Katsuta,[3] J. Knödlseder,[48,49] M. Kuss,[11] J. Lande,[3] S. Larsson,[29,30,50] L. Latronico,[51] M. Lemoine-Goumard,[52,53] F. Longo,[6,7] F. Loparco,[15,16] M. N. Lovellette,[37] P. Lubrano,[12,13] G. M. Madejski,[3] F. Massaro,[3] M. Mayer,[1] M. N. Mazziotta,[16] J. E. McEnery,[14,54] J. Mehault,[27] P. F. Michelson,[3] R. P. Mignani,[55] W. Mitthumsiri,[3] T. Mizuno,[56] A. A. Moiseev,[20,54] M. E. Monzani,[3] A. Morselli,[57] I. V. Moskalenko,[3] S. Murgia,[3] T. Nakamori,[47] R. Nemmen,[14] E. Nuss,[27] M. Ohno,[58] T. Ohsugi,[56] N. Omodei,[3] M. Orienti,[39] E. Orlando,[3] J. F. Ormes,[59] D. Paneque,[3,60] J. S. Perkins,[14,21,20,61] M. Pesce-Rollins,[11] F. Piron,[27] G. Pivato,[10] S. Rainò,[15,16] R. Rando,[9,10] M. Razzano,[11,62] S. Razzaque,[22] A. Reimer,[3,63] O. Reimer,[3,63] S. Ritz,[62] C. Romoli,[10] M. Sánchez-Conde,[3] A. Schulz,[1] C. Sgrò,[11] P. E. Simeon,[3] E. J. Siskind,[64] D. A. Smith,[52] G. Spandre,[11] P. Spinelli,[15,16] F. W. Stecker,[14,65] A. W. Strong,[66] D. J. Suson,[67] H. Tajima,[3,68] H. Takahashi,[38] T. Takahashi,[58] T. Tanaka,[3,69]* J. G. Thayer,[3] J. B. Thayer,[3] D. J. Thompson,[14] S. E. Thorsett,[70] L. Tibaldo,[9,10] O. Tibolla,[71] M. Tinivella,[11] E. Troja,[14,72] Y. Uchiyama,[3]* T. L. Usher,[3] J. Vandenbroucke,[3] V. Vasileiou,[27] G. Vianello,[3,73] V. Vitale,[57,74] A. P. Waite,[3] M. Werner,[63] B. L. Winer,[44] K. S. Wood,[37] M. Wood,[3] R. Yamazaki,[75] Z. Yang,[29,30] S. Zimmer[29,30]

Cosmic rays are particles (mostly protons) accelerated to relativistic speeds. Despite wide agreement that supernova remnants (SNRs) are the sources of galactic cosmic rays, unequivocal evidence for the acceleration of protons in these objects is still lacking. When accelerated protons encounter interstellar material, they produce neutral pions, which in turn decay into gamma rays. This offers a compelling way to detect the acceleration sites of protons. The identification of pion-decay gamma rays has been difficult because high-energy electrons also produce gamma rays via bremsstrahlung and inverse Compton scattering. We detected the characteristic pion-decay feature in the gamma-ray spectra of two SNRs, IC 443 and W44, with the Fermi Large Area Telescope. This detection provides direct evidence that cosmic-ray protons are accelerated in SNRs.

A supernova explosion drives its progenitor material supersonically into interstellar space, forming a collisionless shock wave ahead of the stellar ejecta. The huge amount of kinetic energy released by a supernova, typically 10^{51} ergs, is initially carried by the expanding ejecta and is then transferred to kinetic and thermal energies of shocked interstellar gas and relativistic particles. The shocked gas and relativistic particles produce the thermal and nonthermal emissions of a supernova remnant (SNR). The mechanism of diffusive shock acceleration (DSA) can explain the production of relativistic particles in SNRs (*1*). DSA generally predicts that a substantial fraction of the shock energy is transferred to relativistic protons. Indeed, if SNRs are the main sites of acceleration of the galactic cosmic rays, then 3 to 30% of the supernova kinetic energy must end up transferred to relativistic protons. However, the presence of relativistic protons in SNRs has been mostly inferred from indirect arguments (*2*–*5*).

A direct signature of high-energy protons is provided by gamma rays generated in the decay of neutral pions (π^0); proton-proton (more generally nuclear-nuclear) collisions create π^0 mesons, which usually quickly decay into two gamma rays (*6*–*8*) (schematically written as $p + p \rightarrow \pi^0 +$ other products, followed by $\pi^0 \rightarrow 2\gamma$), each having an energy of $m_{\pi^0}c^2/2 = 67.5$ MeV in the rest frame of the neutral pion (where m_{π^0} is the rest mass of the neutral pion and c is the speed of light). The gamma-ray number spectrum, $F(\varepsilon)$, is thus symmetric about 67.5 MeV in a log-log representation (*9*). The π^0-decay spectrum in the usual $\varepsilon^2 F(\varepsilon)$ representation rises steeply below ~200 MeV and approximately traces the energy distribution of parent protons at energies greater than a few GeV. This characteristic spectral feature (often referred to as the "pion-decay bump") uniquely identifies π^0-decay gamma rays and thereby high-energy protons, allowing a measurement of the source spectrum of cosmic rays.

Massive stars are short-lived and end their lives with core-collapse supernova explosions. These explosions typically occur in the vicinity of molecular clouds with which they interact. When cosmic-ray protons accelerated by SNRs penetrate into high-density clouds, π^0-decay gamma-ray emission is expected to be enhanced because of more frequent *pp* interactions relative to the interstellar medium (*10*). Indeed, SNRs

Science

Similarity of Scattering Rates in Metals Showing *T*-Linear Resistivity

J. A. N. Bruin, H. Sakai, R. S. Perry and A. P. Mackenzie

Science **339** (6121), 804-807.
DOI: 10.1126/science.1227612

Quantum Critical Scattering

The temperature (T) dependence of the electrical resistivity offers clues about the behavior of electrical carriers. One of the more puzzling observations is the T-linear resistivity found in systems known or suspected to exhibit quantum criticality, such as cuprate and organic superconductors, and heavy fermion materials; the origin of this behavior remains elusive. **Bruin *et al.*** (p. 804) find that the ruthenate $Sr_3Ru_2O_7$ also exhibits T-linear resistivity in the vicinity of its quantum critical point, and that its scattering rate per kelvin is approximately given by the inverse of a characteristic time made up of the Planck and Boltzmann constants. A comprehensive analysis of other systems with T-linear resistivity, including ordinary metals at high temperatures, indicates that their scattering rates are similarly close to the characteristic rate. That the rates are similar across a wide range of materials with diverse microscopic scattering mechanisms may indicate universal behavior.